THE JOURNAL OF PHYSICAL CHEMISTRY B

Article

pubs.acs.org/JPCB

Ion-Specific Modulation of Interfacial Interaction Potentials between Solid Substrates and Cell-Sized Particles Mediated via Zwitterionic, Super-Hydrophilic Poly(sulfobetaine) Brushes

Yuji Higaki,[†,‡,#] Benjamin Fröhlich,[§,#] Akihisa Yamamoto,[∥] Ryo Murakami,[⊥] Makoto Kaneko,[⊥] Atsushi Takahara,[*,†,‡] and Motomu Tanaka[*,§,∥]

[†]Institute for Materials Chemistry and Engineering, Kyushu University, 744 Motooka, Nishi-ku, Fukuoka 819-0395, Japan

[‡]International Institute for Carbon-Neutral Energy Research (WPI I2CNER), Kyushu University, 744 Motooka, Nishi-ku, Fukuoka 819-0395, Japan

[§]Physical Chemistry of Biosystems, University of Heidelberg, D69120 Heidelberg, Germany

[∥]Institute for Integrated Cell-Material Sciences (WPI iCeMS), Kyoto University 606-8501 Kyoto, Japan

[⊥]Department of Mechanical Engineering, Osaka University, 565-0871 Suita, Japan

Supporting Information

ABSTRACT: Zwitterionic polymer brushes draw increasing attention not only because of their superhydrophilic, self-cleaning capability but also due to their excellent antifouling capacity. We investigated the ion-specific modulation of the interfacial interaction potential via densely packed, uniform poly(sulfobetaine) brushes. The vertical Brownian motion of a cell-sized latex particle was monitored by microinterferometry, yielding the effective interfacial interaction potentials $V(\Delta h)$ and the autocorrelation function of height fluctuation. The potential curvature $V''(\Delta h)$ exhibited a monotonic increase according to the increase in monovalent salt concentrations, implying the sharpening of the potential confinement. An opposite tendency was observed in $CaCl_2$ solutions, suggesting that the ion specific modulation cannot be explained by the classical Hofmeister series. When the particle fluctuation was monitored in the presence of free sulfobetaine molecules, the increase in [sulfobetaine] resulted in a distinct increase in hydrodynamic friction. This was never observed in all the other salt solutions, suggesting the interference of zwitterionic pairing of sulfobetaine side chains by the intercalation of sulfobetaine molecules into the brush layer. Furthermore, poly(sulfobetaine) brushes exhibited a very low $V''(\Delta h)$ and hydrodynamic friction to human erythrocytes, which seems to explain the excellent blood repellency of zwitterionic polymer materials.

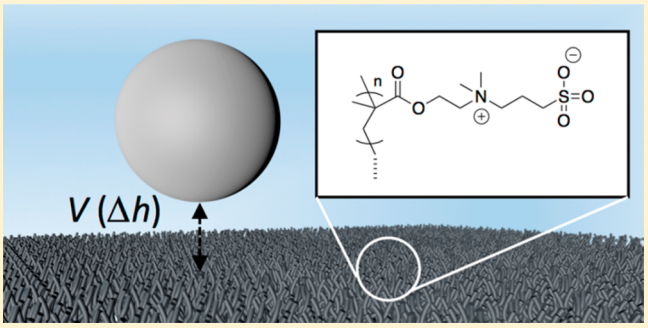

INTRODUCTION

Zwitterionic molecules, a family of molecules that consist of moieties carrying both positive and negative charges, are widely found in nature. For example, cell membranes mainly consist of zwitterionic phospholipids, preventing nonspecific adsorption of proteins to cell surfaces. Phospholipids are derivatives of glycerol (glycerophospholipids) or sphingosine (sphingophospholipids), among which phosphatidylcholine and sphingomyelin rendered with zwitterionic phosphocholine (or phosphobetaine) moieties make up more than 50% of total lipids in most animal tissues.[1,2] A number of reports evidenced that the misbalance in phospholipid composition is strongly correlated with diseases, such as pronounced clotting of sickled erythrocytes.[3]

Zwitterionic polymers have been inspiring material scientists as a promising alternative to commonly used, nonionic oligoethylene glycols that can fulfill various industrial demands, such as self-cleaning and antifouling capabilities.[4−7] Compared to the grafting of polymer chains from solutions ("grafting onto" method) or physisorption of block copolymers from the solution,[8] the surface-initiated controlled chain growth (also called the "grafting from" method) enables the formation of highly dense, defect-free polymer brush layers.[9] The zwitterionic polymer brushes exhibit unique hydration behaviors due to the interchain paring of zwitterions, also referred to as "antielectrolyte effects". For example, the hydration radius of poly(phosphocholine) showed no dependence on ionic strength, while that of poly(sulfobetaine) significantly increased at high NaCl concentrations.[10,11] Moreover, quartz crystal microbalance with dissipation (QCM-D) study further suggested different responses of poly(sulfobetaine) brushes to anions.[12] To date, excellent antifouling performance of

Received: November 16, 2016
Revised: January 25, 2017
Published: January 25, 2017

DOI: 10.1021/acs.jpcb.6b11540
J. Phys. Chem. B 2017, 121, 1396−1404

zwitterionic polymer brushes is attributed to the excluded volume effect and the lower free energy gain through the foulant adsorption.[5] Such unique hydration characteristics of zwitterionic polymer brushes can also be correlated with extremely low dynamic frictional coefficients,[12−16] exhibiting the hydrodynamic lubrication state under aqueous condition at high sliding velocity regime. However, despite a variety of potential applications in biomaterial sciences, little is understood how the zwitterionic polymer brushes modulate the interfacial potentials in the presence of ions.

Recently, we reported the fine-adjustment of interfacial interaction potentials between latex particles and contact substrates via pH responsive hydrogels.[17] In this study, we further extended this strategy to unravel how ions influence the vertical Brownian motion of cell-sized latex particles (diameter $\Phi \sim 10\ \mu m$) and osmotically tensed human erythrocytes that hover on the zwitterionic polymer brush surface (Scheme 1).

Scheme 1. Schematic Illustration of Experimental System[a]

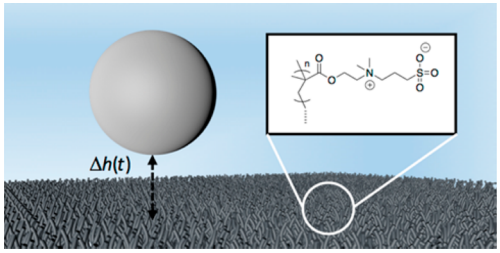

[a]Height fluctuation of the particle $\Delta h(t)$ is monitored by reflection interference contrast microscopy (RICM).

Glass substrates were coated with poly(sulfobetaine) brushes, and the height fluctuation of particles/cells was precisely determined by using a label-free reflection interference contrast microscopy (RICM).[18−20] The vertical Brownian motion of a particle can be described by the Langevin equation, which can analytically be solved by several assumptions, such as damping of particle motion and harmonic interaction potential. Under thermodynamic equilibrium, the probability function of fluctuation amplitude $P(\Delta h)$ can be used to calculate the effective interfacial potential $V(\Delta h)$.[21] A special focus of this study is to shed light on the ion specific modulation of interfacial potentials in the presence of three different monovalent cations (Na^+, K^+, and $N(CH_3)_4^+$) and a divalent cation (Ca^{2+}) without changing the counterion (Cl^-). The influence of antielectrolyte effect (zwitterionic pairing of sulfobetaine side chains) was also examined by dissolving free sulfobetaine molecules in the medium. Finally, we tracked the vertical Brownian motion of human erythrocytes. The details of experimental findings are explained in the following sections.

MATERIALS AND METHODS

Materials. Milli-Q water (Millipore Inc., Billerica, MA) was used throughout the study. Unless stated otherwise, all chemicals were purchased from Wako Pure Chemical Industries (Osaka, Japan), Merck (Darmstadt, Germany), Carl Roth (Karlsruhe, Germany) or Sigma-Aldrich (Neu-Ulm, Germany), and used without further purification. Latex particles of 5 μm radius and 1.04 g/cm^3 density were purchased from Macherey-Nagel (Düren, Germany). Adult blood was drawn from healthy donors under the approval of the Joint Ethics Committee of IFLMS, iCeMS, and CiRA, Kyoto University. Poly(sulfobetaine) (poly[3-(*N*-2-methacryloyloxyethyl-*N*,*N*-dimethyl)ammonatopropanesulfonate]) brushes were prepared by surface-initiated atom transfer radical polymerization on glass plate (25 mm × 40 mm).[22] Details of the preparation procedures and reaction conditions were described in the Supporting Information (SI).

Atomic Force Microscopy (AFM). Thickness and the surface roughness of hydrated polymer brushes were measured by Cypher ES AFM (Asylum Research, Santa Barbara, CA), using a pyramidal Si_3N_4 cantilever (OMCL-TR800PSA, Olympus Corporation, Tokyo, Japan; spring constant: 0.57 N m^{-1}, tip radius: less than 20 nm). Topographic images were obtained in contact mode at 298 K, and scratch tracks made by sharp needles were used to determine the film thickness both in ambient atmosphere and in buffer solutions. As the buffer solutions, we used 10 mM HEPES (4-(2-hydroxyethyl)-1-piperazin ethane sulfuric acid) mixed with NaCl, KCl, $CaCl_2$, $N(CH_3)_4Cl$, or nondetergent sulfobetaine (NDSB-195) at concentrations of 1.5 mM, 15 mM, or 150 mM. pH was adjusted to 7.4 by titration with 1.0 M NaOH, 1.0 M KOH, saturated $Ca(OH)_2$, and NH_4OH aqueous solution, respectively. For each measurement, the root-mean-square (RMS) roughness was obtained from 5 μm × 5 μm scanning area.

Reflection Interference Contrast Microscopy (RICM). Prior to the height fluctuation analysis of latex particles, the latex particles were incubated in 1 mg/mL bovine serum albumin (BSA) solution for 15 min to avoid nonspecific adhesion. For the height fluctuation analysis of human erythrocytes, we used 83 mM NaCl (pH 6.4) to deform them into spherocytes.[23] All the fluctuation experiments were carried out at 298 K, using an Axio Observer Z1 microscope (Zeiss, Oberkochen, Germany) equipped with an oil immersion objective lens (NA 1.25, 63 ×, PH3). A monochromatic light from a high-pressure metal halide lamp (λ = 546 nm) was selected with a band-pass filter for the observation. Two polarizers were inserted into the light path in orthogonal arrangement: one was placed in the illumination and the other in the detection path. A quarter-wave plate was inserted behind the front lens of the objective, and the Illumination Numerical Aperture (INA) was adjusted to 0.48 to record multiple interferences. 1000−2000 consecutive images were accumulated with an Orca-Flash4.0LT camera (Hamamatsu Photonics, Herrsching, Germany) at an exposure time of 30 ms, and were subjected to the analysis.

Data Analysis. The artifact from the lateral drift of particles was minimized by applying an edge detection filter to each image. After the radial integration, two consecutive maximum/minimum positions (E1, E2) closest to the center were selected. Under a quasi-normal light incidence, the simplified theory can be applied to perform the conversion of intensity I to relative height Δh_{pp} for all pixel positions (pp) in between E1 and E2:[24]

$$\frac{2I_{pp} - (I_{E1} + I_{E2})}{I_{E1} - I_{E2}} = \cos\left(4\pi n_{buffer}\frac{\Delta h_{pp}}{\lambda}\right) \quad (1)$$

Δh_{pp} was calculated for all frames and used to obtain the relative bead position $\Delta h = \Delta h_{pp} - \langle \Delta h_{pp} \rangle$. All analyses were performed using self-written routines in Matlab (R2014b).

Theoretical Background. The equation of motion for a latex particle undergoing vertical Brownian motion in the interfacial potential $V(\Delta h)$ can be given by a Langevin equation:

DOI: 10.1021/acs.jpcb.6b11540
J. Phys. Chem. B 2017, 121, 1396−1404

$$m\frac{\partial^2\Delta h}{\partial t^2} + \gamma\frac{\partial\Delta h}{\partial t} + \frac{\partial V}{\partial\Delta h} = F_{\text{stoch}} \quad (2)$$

where m is the mass of a particle, γ the friction coefficient, Δh the relative particle position, and F_{stoch} represents the stochastic force of the thermal noise. The second term is the frictional force F_{fric} that can be written by the Reynolds equation:[25]

$$F_{\text{fric}} = \gamma\frac{\partial\Delta h}{\partial t}, \quad \text{where} \quad \gamma = 6\pi\eta_{\text{eff}}\frac{R^2}{h} \quad (3)$$

where $\frac{\partial\Delta h}{\partial t}$ is the relative velocity, η_{eff} is the effective shear viscosity of the system, and h is the absolute distance between the particle and the surface. From the bead radius $R \approx 5$ μm, $\frac{\partial\Delta h}{\partial t} \approx \frac{10^{-8}}{0.03}$ m/s, the density of latex particle $\rho = 1.04$ g/cm^3, and the viscosity of water $\eta_w = 1$ mN m^{-2} s, the estimated Reynolds number Re of the system,[25] $\text{Re} \leq R\left(\frac{\partial\Delta h}{\partial t}\right)\rho\eta_w^{-1} \sim 10^{-4}$, is far below 1. Here, the particle movement is overdamped, and thus the first acceleration term in the Langevin equation (eq 2) is negligible.[26] Moreover, in case the amplitude of height fluctuation is small, the effective interfacial potential can be approximated as harmonic:[27]

$$V(\Delta h) = \frac{1}{2}\frac{\partial^2 V}{\partial\Delta h^2}\bigg|_{\langle h\rangle_t}(\Delta h - \langle\Delta h\rangle)^2 = \frac{1}{2}V''\Delta h^2 \quad (4)$$

The amplitude of fluctuation in our experimental system is $\Delta h \leq 30$ nm, which enables one to analytically solve the Langevin equation. The autocorrelation function of height fluctuation can be calculated within the framework of the fluctuation−dissipation theorem:

$$\langle\Delta h(\delta t)\Delta h(0)\rangle \approx \langle\Delta h^2(0)\rangle e^{-\delta t/\tau},$$
$$\text{where} \quad \tau = \frac{\gamma}{V''} = \frac{6\pi\eta_{\text{eff}}R^2}{\langle h\rangle V''} \quad (5)$$

Here the mean squared amplitude can be derived from the equipartition theorem:

$$\langle\Delta h^2(0)\rangle = \frac{k_BT}{V''} \quad (6)$$

Under thermodynamic equilibrium, the effective interfacial potential $V(\Delta h)$ can also be calculated from the probability function of fluctuation amplitude of the particle $P(\Delta h)$, following Boltzmann's distribution:[18−20]

$$P(\Delta h) \propto \exp\left(-\frac{V(\Delta h)}{k_BT}\right) \quad \text{and thus}$$
$$V(\Delta h) = -k_BT\ln(P(\Delta h)) + \text{const} \quad (7)$$

RESULTS

Basic Characterization of Poly(sulfobetaine) Brushes. Figure 1 represents the topographic profiles (upper panels) and the corresponding height profiles (lower panels) of poly(sulfobetaine) brushes obtained by contact mode AFM, measured (a) in ambient atmosphere and (b) in 150 mM NaCl buffered with 10 mM HEPES (pH 7.4). To determine the film thickness, the right part of the sample was scratched by a high force. Although a few debris were observed in the scratched region, we confirmed that the flat "ground" region corresponds to the bare substrate by comparing the mechanical response of the cantilever from two regions in tapping mode AFM phase lag imaging (Supporting Information Figure S1). The root mean squared (RMS) roughness of the dry film lies around 0.5 nm even over a large scan area (5×5 μm^2), confirming that the poly(sulfobetaine) brushes form a homogeneous, molecularly smooth surface. According to the hydration in bulk electrolyte, the film thickness increases from 54 to 112 nm. Moreover, we carried out the AFM imaging while keeping the tip deflection minimum in order to guarantee the reproducible topographic profiles. It is notable that the hydration does not cause a roughening of the surfaces, owing to the uniform degree of polymerization achieved by surface-initiated controlled radical polymerization. The data measured for different concentrations and different ions are summarized in Table 1.

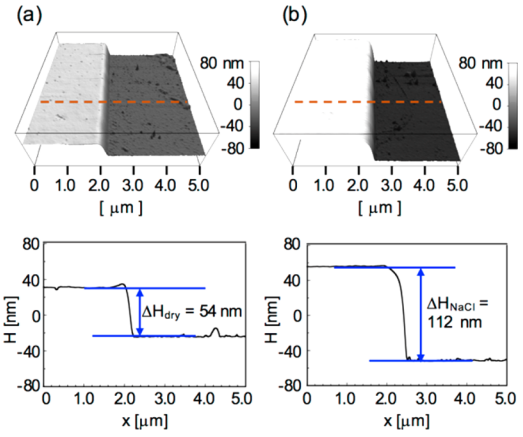

Figure 1. AFM images of poly(sulfobetaine) brushes measured (a) in ambient atmosphere and (b) in 150 mM NaCl buffered with 10 mM HEPES (pH 7.4). The lower panels represent the line profiles along the broken lines in upper panels. RMS roughness of the film remains almost constant around 0.5 nm even after full hydration.

Height Fluctuation as a Function of NaCl Concentration. Figure 2a represents successive RICM snapshots of a latex particle in 15 mM NaCl buffered with 10 mM HEPES (pH 7.4). The time interval between the successive images in the figure is 0.6 s. Figure 2b1 shows the range of intensity profiles obtained by simple line scans (light gray area), the mean radial intensity profile after azimuthal integration (data points and black line), and the intensity values within the standard deviation of the mean radial intensity (dark gray area). Utilizing the mean radial intensity profiles increases the accuracy of the analysis and is therefore used, unless stated otherwise.

Figure 3a represents the height fluctuation of a latex particle $\Delta h(t)$ in NaCl recorded over 30 s. The latex particle exhibited a rigorous height fluctuation $\Delta h(t)$ in 1.5 mM NaCl, whose fluctuation amplitude was found to be $\pm$10 nm. An increase in [NaCl] led to a distinct damping of height fluctuation. In fact, the height fluctuation is confined mostly within $\pm$5 nm at [NaCl] = 150 mM. The corresponding effective interfacial potentials normalized by the thermal energy, $V(\Delta h)/k_BT$, are plotted in Figure 3b. The interfacial potentials near the minimum $\Delta h = 0$ can be well approximated as harmonic potentials, confirming the validity of Derjaguin's approximation of weak and thus nonspecific interactions.[27,28] As indicated by arrows in Figure 3b, the potential curvature of parabola or the spring constant of harmonic potential $V''(\Delta h)$ shows a

DOI: 10.1021/acs.jpcb.6b11540
J. Phys. Chem. B 2017, 121, 1396−1404

Table 1. Summary of AFM Film Characterization[a]

	thickness [nm]				RMS roughness [nm]			
c [mM]	KCl	NaCl	$N(CH_3)_4Cl$	$CaCl_2$	KCl	NaCl	$N(CH_3)_4Cl$	$CaCl_2$
1.5	96	102	93	100	0.5	0.5	0.7	0.7
15	110	101	90	101	0.5	0.5	0.6	0.8
150	110	112	112	121	1.0	0.5	0.8	1.4

[a]All topographic data were taken by the same poly(sulfobetaine) brush film with a thickness in ambient atmosphere ΔH_{dry} = 54 nm.

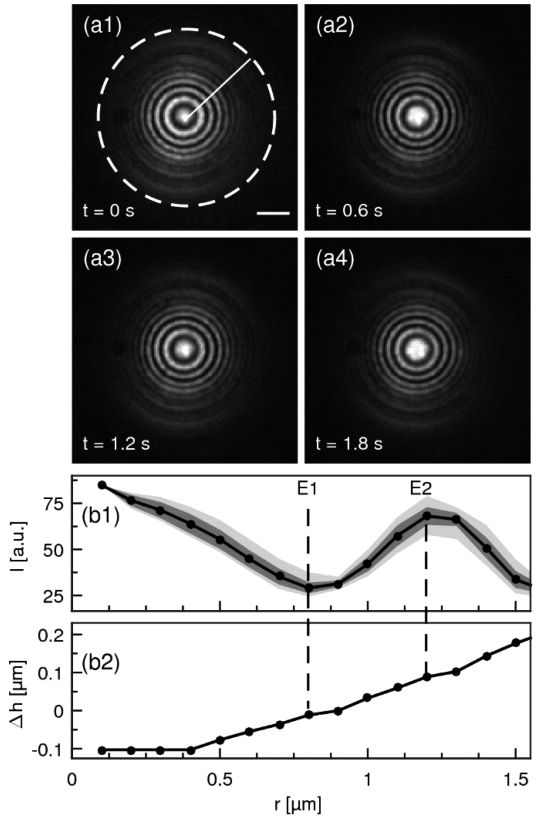

Figure 2. (a) Successive RICM snapshots of a latex particle hovering on the surface of poly(sulfobetaine) brush. Electrolyte: 15 mM NaCl buffered with 10 mM HEPES, pH 7.4. Time interval between the pictures: 0.6 s. Scale bar: 2 μm. (a1) Solid line represents a typical line scan. Azimuthal integration of line scans is performed over the circle indicated by the dashed line. (b1) Range of radial intensity profiles obtained by single line scans (light gray area), mean radial intensity (data points and black line), and the intensity values within the standard deviation of the mean intensity (dark gray area). (b2) The relative height profile calculated with eq 1.

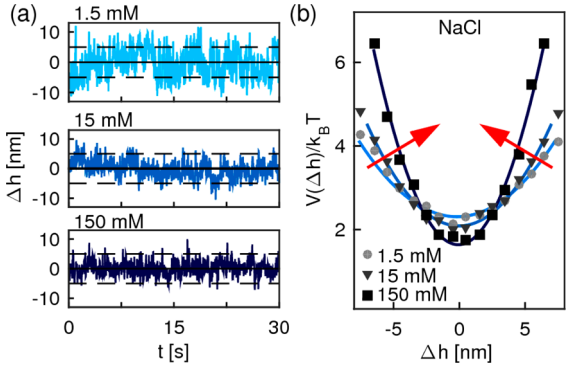

Figure 3. (a) Height fluctuations of latex particles $\Delta h(t)$ recorded over 30 s in 1.5 mM, 15 mM, and 150 mM NaCl. Damping of the vertical Brownian motion of the particle was most pronounced in 150 mM NaCl. (b) The normalized effective interfacial interaction potentials $V(\Delta h)/k_BT$. Solid lines coincide with the fitting based on a harmonic assumption (eq 4). The direction of increases in salt concentration is indicated by arrows.

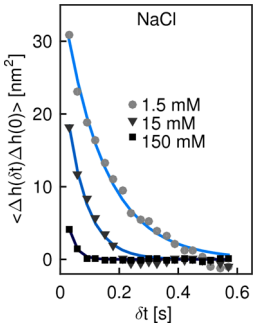

Figure 4. Autocorrelation function of height fluctuation calculated for different NaCl concentrations. Solid lines indicate single exponential fits.

monotonic increase according to the increase in [NaCl], indicating that the latex particle is more sharply confined in the potential well at higher [NaCl].

Figure 4 represents the autocorrelation functions of height fluctuation calculated for different [NaCl]. As indicated by solid lines, the correlation functions can be well fitted as single exponential functions (eq 5). It was found that the increase in [NaCl] leads to a distinct decrease in the mean squared amplitude of fluctuation $\langle \Delta h^2(0) \rangle$ (eq 6) and the characteristic relaxation time τ. The increase in [NaCl] from 1.5, 15, to 150 mM is followed by the decrease in $\langle \Delta h^2(0) \rangle$ from 210, 86, to 8 nm^2, reflecting the damping of vertical Brownian motion. On the other hand, we found a monotonic decrease in τ from 0.13 s, 0.08 s, to 0.05 s according to the increase in [NaCl] from 1.5 mM, 15 mM, to 150 mM, respectively. It is notable that the change in [NaCl] caused no detectable change in the hydrodynamic friction γ.

Ion-Specific Modulation of Interfacial Potentials. Can the modulation of interfacial potentials only be the matter of ionic strength? Or, do ionic species also matter? To address this point, we selected two monovalent salts with Cl^- counterion, KCl and $N(CH_3)_4Cl$, and performed experiments along the same line. K^+ is the neighboring ion to Na^+ in the classical Hofmeister series,[29] while $N(CH_3)_4^+$ is located at the Kosmotrope side. Figure 5 represents the normalized effective interfacial potentials $V(\Delta h)/k_BT$ (left panels) and the corresponding autocorrelation functions of height fluctuation (right panels) of poly(sulfobetaine) brushes in (a) KCl and (b) $N(CH_3)_4Cl$ buffered with 10 mM HEPES (pH 7.4). Similar to those in NaCl (Figure 3b), the normalized potentials can be well approximated as harmonic ones. The global shapes of potentials in KCl (Figure 5b) are similar to those in NaCl. At [KCl] = 1.5 mM and 15 mM, the height fluctuation of the latex

DOI: 10.1021/acs.jpcb.6b11540
J. Phys. Chem. B 2017, 121, 1396−1404

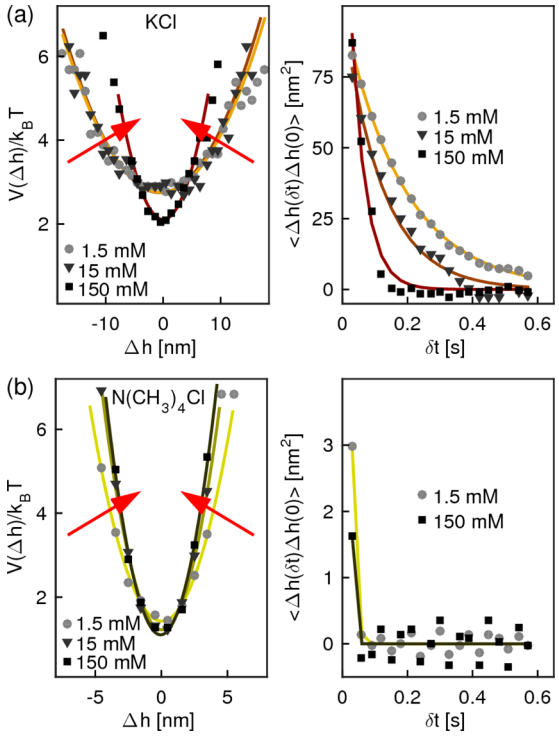

Figure 5. Normalized effective interfacial interaction potentials $V(\Delta h)/k_BT$ (left panels) and the autocorrelation function of height fluctuations (right panels) calculated for (a) KCl and (b) $N(CH_3)_4Cl$. Note that the *x*-axis range in the left panel of (a) is different from other buffer conditions to present the large height fluctuation. The directions of increase in salt concentration are indicated by arrows.

particles (Supporting Information, Figure S2) is slightly more pronounced than in NaCl, but the fluctuation amplitude sharply dropped at [KCl] = 150 mM. Such a tendency is correlated with the decrease in the mean squared amplitude of fluctuation $\langle \Delta h^2(0) \rangle$ as well as the relaxation time τ, as found in NaCl solutions (Figure 4). In contrast, the height fluctuation of latex particles in $N(CH_3)_4Cl$ was much smaller (Figure 5b). For example, the fluctuation amplitudes (SI) at 1.5 mM and 15 mM $N(CH_3)_4Cl$ were about 2−3 times smaller than the corresponding conditions in NaCl and KCl, implying that the particles are sharply confined near the potential minima even at very low salt concentrations. Further increase in salt concentration to 150 mM did not cause a major change in the potential. The spring constant V'' in $N(CH_3)_4Cl$, $\sim 20 \times 10^{-22}$ J nm^{-2}, were almost an order of magnitude higher than the corresponding values of Na^+ and K^+. Nevertheless, the increase in $[N(CH_3)_4Cl]$ led to the increase in V'' and decrease in $\langle \Delta h^2(0) \rangle$, showing the same tendency as in NaCl and KCl.

These experimental findings led to the next question. Does the valency of cations play any role? To address this point, we performed the experiments in $CaCl_2$ (Figure 6), which has a divalent Ca^{2+} but the same Cl^-. Although the thickness and RMS roughness values of poly(sulfobetaine) brushes in $CaCl_2$ are comparable to the corresponding values obtained for all the monovalent cations (Table 3), the height fluctuation of latex particle was sharply confined within ±5 nm in 1.5 mM $CaCl_2$ (SI), which is clearly different from what we observed in NaCl and KCl. In fact, the spring constant V'' at $[CaCl_2]$ = 1.5 mM is comparable to that in $N(CH_3)_4Cl$, $\sim 20 \times 10^{-22}$ J nm^{-2}. However, in contrast to the results in $N(CH_3)_4Cl$, we observed a remarkable decrease in V'' by more than the factor of 2 by

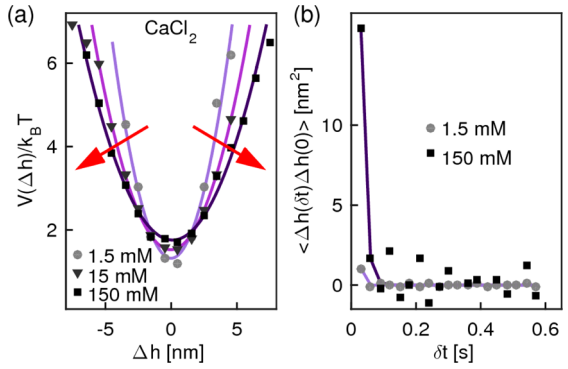

Figure 6. (a) Normalized effective interfacial interaction potential $V(\Delta h)/k_BT$ and (b) autocorrelation function of height fluctuation calculated for $CaCl_2$. Note that V'' decreases according to the increase in $[CaCl_2]$, corresponding to a "softening" of the interfacial potential. Changes in the potential curvature by increasing salt concentrations (indicated by arrows) were opposite to the results presented in Figure 3 and Figure 5.

increasing $[CaCl_2]$ from 1.5 mM to 150 mM, implying the "softening" of interfacial potentials by the increase in $[CaCl_2]$. The overall tendency, the decrease in potential confinement by increasing salt concentrations, is opposite to what we observed in the monovalent salt solutions, suggesting that the interactions of divalent Ca^{2+} is different from monovalent cations.

Influence of Zwitterion Pairing. Ample evidence indicated, either directly or indirectly, that the unique material characteristics of zwitterionic polymer brushes originate from the interchain pairing of side chains (antielectrolyte effect).[5,12] Therefore, we performed the experiments in the presence of nondetergent sulfobetaine in solutions to examine whether the interchain pairing could be interfered by the presence of "competitors" that are identical to the side chains. As presented in Figure 7a, an increase in V'' and thus a sharpening of the harmonic potential according to the increase in [sulfobetaine] seems qualitatively similar to the tendency observed for the monovalent salts. It should be noted that the mean square amplitude of height fluctuation $\langle \Delta h^2(0) \rangle$ in the presence of nondetergent sulfobetaine in solutions was almost an order of magnitude smaller than in KCl and NaCl solutions (Table 3). Consequently, the V'' values in sulfobetaine solution are much higher than those in NaCl and KCl, reflecting the damping of vertical Brownian motion. Interestingly, the autocorrelation function analysis (Figure 7b) showed no remarkable change in τ at elevated [sulfibetaine] (Table 3). Since $\gamma = V''\tau$ (eq 5), the combination of an increase in V'' at constant τ results in an increase in hydrodynamic friction coefficient γ according to the increase in [sulfibetaine] (eq 5), suggesting that sulfobetaine molecules disturb the zwitterionic pairing between the side chains by intercalating into the brush layer.

DISCUSSION

Influence of Ionic Strength and Ion Specificity. A previous light scattering study[8] suggested that the hydrodynamic radius of poly(sulfobetaine) monotonically increases as a function of [NaCl] beyond the theta concentration (c^* = 74 mM). This finding qualitatively agrees well with specular neutron reflectivity results,[9] suggesting that the brush-electrolyte interface becomes more diffusive at [NaCl] > c^*. The density profiles of poly(sulfobetaine) brushes suggest the

DOI: 10.1021/acs.jpcb.6b11540
J. Phys. Chem. B 2017, 121, 1396−1404

Table 2. Summary of V'', τ, and γ for NaCl, KCl, and $N(CH_3)_4Cl$[a]

	c [mM]	MSA [nm^2]	V'' [10^{-22} J/nm^2]	τ [s]	γ [10^{-22} Js/nm^2]
NaCl	1.5	210 ± 89	2 ± 1	0.13 ± 0.07	0.28 ± 0.17
	15	86 ± 49	3 ± 1	0.08 ± 0.03	0.27 ± 0.11
	150	8 ± 3	7 ± 2	0.05 ± 0.02	0.30 ± 0.18
KCl	1.5	160 ± 80	1 ± 0.5	0.20 ± 0.01	0.23 ± 0.05
	15	130 ± 72	1 ± 0.5	0.16 ± 0.03	0.19 ± 0.04
	150	75 ± 33	4 ± 1	0.03 ± 0.01	0.11 ± 0.03
$N(CH_3)_4Cl$	1.5	6 ± 4	17 ± 4	0.01 ± 0.01	0.15 ± 0.12
	15	3 ± 2	21 ± 4	<0.01	<0.1
	150	3 ± 2	23 ± 4	<0.01	<0.1

[a]Note that $\tau \approx 0.01$ is the instrumental resolution (e.g., Figure 5b, right panel).

Table 3. Summary of V'', τ, and γ for $CaCl_2$ and Sulfobetaine

	c [mM]	MSA [nm^2]	V'' [10^{-22} J/nm^2]	τ [s]	γ [10^{-22} Js/nm^2]
$CaCl_2$	1.5	2 ± 1	25 ± 5	<0.01	<0.1
	15	3 ± 1	15 ± 4	<0.01	<0.1
	150	5 ± 2	10 ± 2	0.01 ± 0.01	0.1 ± 0.1
sulfobetaine	1.5	10 ± 4	6 ± 2	0.04 ± 0.01	0.18 ± 0.15
	15	10 ± 4	7 ± 3	0.04 ± 0.01	0.2 ± 0.09
	150	6 ± 3	12 ± 4	0.03 ± 0.01	0.28 ± 0.14

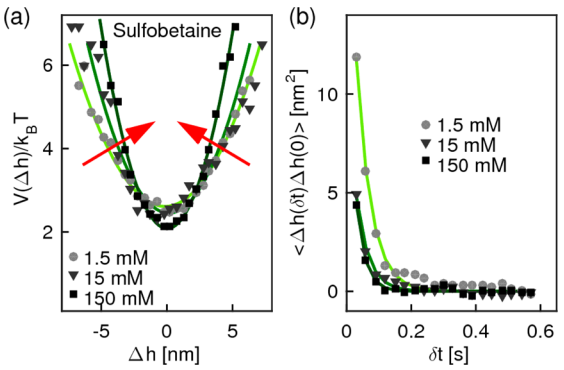

Figure 7. (a) Normalized effective interfacial interaction potential $V(\Delta h)/k_BT$ and (b) autocorrelation function of height fluctuation in sulfobetaine solutions. Note that V'' increases according to the increase in sulfobetaine concentration, suggesting that the hydrodynamic friction is strongly damped at higher sulfobetaine concentration. The direction of increases in sulfobetaine concentration is indicated by arrows.

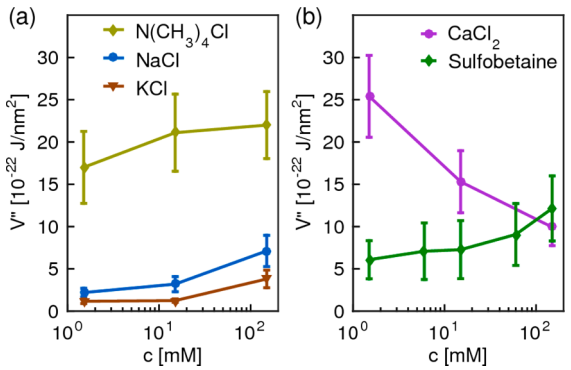

Figure 8. Summary of $V''(\Delta h)$ plotted as a function of salt concentration. (a) KCl, NaCl, and $N(CH_3)_4Cl$ exhibited a clear increase in the sharpness of potential confinement, while (b) $CaCl_2$ showed an opposite tendency. Note that the tendency does not follow a typical Hofmeister series for cations.

coexistence of a poorly swollen inner layer and a highly swollen diffusive layer. This finding is, however, in clear contrast to poly(phosphocholine) brushes that exhibited no change in hydrodynamic radius or density profiles at [NaCl] = 74 mM to 5 M. Currently, it is not possible to explain the different ionic strength dependence of poly(sulfobetaine) and that of poly(phosphobetaine) on the molecular level.

As presented in Figure 3, we found that V'' monotonically increases according to the increase in [NaCl] from 1.5 mM to 150 mM. The prominent increase in V'' observed at [NaCl] = 150 mM suggested the sharpening of the potential at [NaCl] beyond the theta condition (c^* = 74 mM). $N(CH_3)_4Cl$ and KCl exhibited the same tendency, and the V'' values at a given concentration shows a clear sequence; $V''_{KCl} < V''_{NaCl} \ll V''_{N(CH3)4Cl}$ (Figure 8a). As summarized in Table 2, the calculated $V''_{N(CH3)4Cl}$ values are almost by an order of magnitude larger than those for KCl and NaCl.

Since $N(CH_3)_4^+$ is categorized in the group of cationic Kosmotrope,[29] the strongest confinement observed in N-$(CH_3)_4Cl$ naturally draws the next question. Can such an ion specificity be explained by the difference in solvation entropy? K^+ and Na^+ are the neighboring ions in Hofmeister series, and the difference in V'' between these ions is rather minor. Therefore, the comparison with the results in $CaCl_2$ electrolytes helps us address this point. As presented in Figure 8b and Table 3, the V'' value at [$CaCl_2$] = 150 mM is $V''_{CaCl2(150\ mM)} = 10^{-21}$ J/nm^2, which is more than double the values obtained for KCl and NaCl. Moreover, the increase in [$CaCl_2$] resulted in a monotonic "decrease" in V'', which is in contrast to all monovalent salts (Figure 8a). Moreover, the characteristic relaxation time of the height autocorrelation (Figure 8b) was close to the detection limit ($\tau \approx 0.01$ s). These results clearly indicate that monovalent cations and Ca^{2+} interact differently with sulfate groups, such as cross-linking of neighboring sulfate groups.[30] Further extension of this strategy to other divalent cations and ions with higher valencies would help us gain deeper insight into the physical mechanism.

Interestingly, free zwitterionic sulfobetaine molecules in solution influenced the particle fluctuation in a different manner. The increase in [sulfobetaine] led to a monotonic

DOI: 10.1021/acs.jpcb.6b11540
J. Phys. Chem. B 2017, 121, 1396−1404

increase in V'', following the trend observed for monovalent NaCl, KCl, and $N(CH_3)_4Cl$. The absolute $V''_{sulfobetaine}$ level suggests that sulfobetaine confines the particle more sharply in the potential well compared to NaCl and KCl, but this effect is not stronger than $N(CH_3)_4Cl$. Remarkably, the relaxation time τ of height fluctuation showed almost no change even at high sulfobetaine concentrations. As a consequence, the increase in [sulfobetaine] results in a significant increase in the hydrodynamic frictional coefficient from $\gamma_{sulfobetaine(1.5\ mM)} = 18 \times 10^{-22}$ [Js/nm^2] to $\gamma_{sulfobetaine(150\ mM)} = 28 \times 10^{-22}$ [Js/nm^2]. The observed tendency was unique for sulfobetaine solutions, which was not observed in the other salt solutions. Such an increase in hydrodynamic friction according to the increase in [sulfobetaine] suggests the intercalation of sulfobetaine molecules into the poly(sulfobetaine) brush layer, disturbing the original zwitterionic pairs made by the side chains.

Interaction Potentials with Human Erythrocytes. One of the unique characteristics of zwitterionic polymers is their excellent antifouling capability to avoid nonspecific interactions with proteins[31] and lipid vesicles.[32] Recent vibrational spectroscopy studies suggested that such an antifouling function might be attributed to the hydration with "freezing-bound" or "intermediate" water molecules,[33,34] but there has been no quantitative study on the modulation of cell−substrate interactions via zwitterionic polymer brushes. Therefore, we monitored the height fluctuation of human erythrocytes on the surface. Healthy erythrocytes usually take a biconcave shape, and cell membranes undergo rigorous shape fluctuation even in contact with glass substrates.[35] In order to minimize the thermal fluctuation of cell membranes themselves, we osmotically stressed erythrocytes under hypotonic conditions ([NaCl] ∼ 83 mM) and prepared spherical, tense cells. In nature, spherical erythrocytes (called spherocytes) are found in an autohemolytic anemia, called spherocytosis.[36] The use of osmotically tense, spherical erythrocyte (called "osmotic spherocyte" in the following) enables us to minimize the interference caused by the thermal fluctuation of cell membranes. Figure 9a represents a typical RICM snapshot from an osmotic spherocyte on a poly(sulfobetaine) brush substrate. The interference fringes are more diffusive compared to the ones in Figure 2 due to a lower contrast in refractive index. The normalized interfacial potential $V(\Delta h)/k_BT$ (Figure 9c, black) suggests that the cell is trapped in a very shallow potential well. The calculated spring constant $V''_{spherocyte} = 1 \times 10^{-22}$ [J/nm^2] is distinctly lower than that of latex particles in 150 mM NaCl, $V''_{NaCl(150\ mM)} = 7 \times 10^{-22}$ [J/nm^2]. More remarkably, the hydrodynamic friction exerted on osmotic spherocytes is below the detection limit $\gamma_{spherocyte} < 0.1 \times 10^{-22}$ [Js/nm^2]. The control experiments on bare glass substrates (Figure 9c, gray) implied a strong vertical confinement. As summarized in Table 4, the spring constant $V''_{glass} = 10 \times 10^{-22}$ [J/nm^2] and the hydrodynamic friction coefficient $\gamma_{glass} = 0.2 \times 10^{-22}$ [Js/nm^2] on glass confirmed that zwitterionic polymer brushes significantly soften the interfacial interaction potentials. The damping of hydrodynamic friction (Figure 9d), manifesting itself in a very shallow interfacial confinement of human erythrocytes, seems to provide the physical explanation of the previously reported excellent blood repelling capability of zwitterionic polymer brushes.[31] For comparison, the corresponding data set from a discocyte is presented in the Supporting Information (Figure S3).

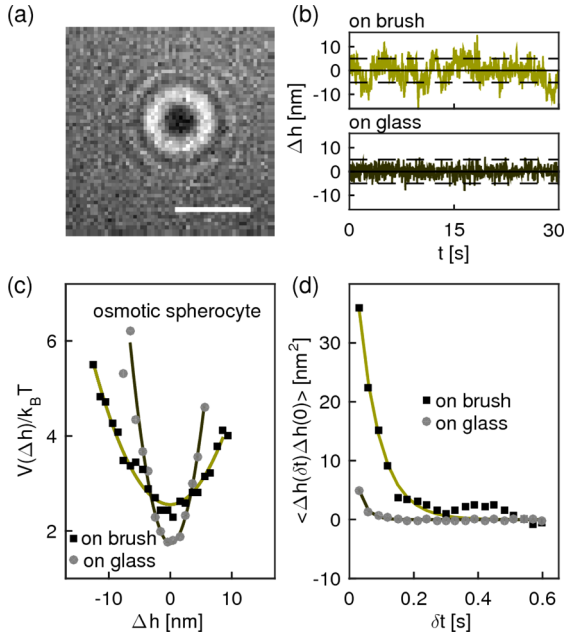

Figure 9. (a) Typical RICM snapshot (scale bar: 2 μm), (b) height fluctuations $\Delta h(t)$, (c) normalized effective potential $V(\Delta h)/k_BT$, and (d) autocorrelation function of height fluctuation of an "osmotic spherocyte" on polymer brush and on glass, in 83 mM NaCl solution. Note that the glass surface was passivated with 1 mg/mL BSA solution for 15 min prior to the experiments to avoid nonspecific cell adhesion.

CONCLUSIONS

We investigated how ions influence the modulation of interfacial potentials between solid substrates and cell models via densely packed, highly uniform poly(sulfobetaine) brushes. In this study, we tracked the fluctuation of the separation distance between the particle and the solid surface using RICM in the presence of three different monovalent cations (Na^+, K^+, and $N(CH_3)_4^+$) and a divalent Ca^{2+} without changing the counterion (Cl^-). The Langevin equation of the particle fluctuation can be solved analytically to gain the interfacial interaction potential $V(\Delta h)$. The spring constant of a harmonic potential V'' monotonically increases according to the increase in monovalent cation concentrations. The V'' values at each concentration always follows a sequence, $V''_{KCl} < V''_{NaCl} \ll V''_{N(CH3)4Cl}$, suggesting that this tendency follows the Hofmeister series. However, the opposite tendency was observed in $CaCl_2$ medium: V'' decreased according to the increase in [$CaCl_2$], and the relaxation time of the autocorrelation of height fluctuation was close to the detection limit ($\tau < 0.01$ [s]). This finding implies that the interaction of poly(sulfobetaine) brushes and the divalent Ca^{2+} is different from those with monovalent cations, suggesting the cross-bridging of anionic sulfate moieties by Ca^{2+}. To gain further insight into the potential contributions of interchain interactions via zwitterion pairing of sulfobetaine side chains, we performed the experiments in the presence of sulfobetaine molecules in solutions. We found that the mean square amplitude of height fluctuations in sulfobetaine solutions were almost 1 order of magnitude smaller than those in KCl and NaCl, implying a sharper potential confinement. Interestingly, the increase in [sulfobetaine] led to a clear increase in the frictional coefficient, which was never observed in the other salt solutions. Such an increase in hydrodynamic friction by increasing [sulfobetaine] suggests the intercalation of sulfobe-

DOI: 10.1021/acs.jpcb.6b11540
J. Phys. Chem. B 2017, 121, 1396−1404

Table 4. Summary of MSA, V'', τ, and γ for Osmotic Spherocytes

substrate	MSA [nm^2]	V'' [10^{-22} J/nm^2]	τ [s]	γ [10^{-22} Js/nm^2]
poly(sulfobetaine) brush	97 ± 103	1 ± 1	0.14 ± 0.09	<0.1
glass	6.6 ± 4.2	10 ± 5	0.02 ± 0.02	0.20 ± 0.19

taine molecules into the brush layer, forming zwitterionic pairs with the side chains. Finally, we examined how poly(sulfobetaine) brushes would mediate the interfacial potential between solid surfaces and biological cells by using "osmotic spherocytes". We found a very shallow potential confinement (small V'') as well as a very low hydrodynamic friction exerted on blood cells, which seem to explain the outstanding blood-repelling capability of zwitterionic brushes. The obtained results demonstrated that the interaction of ions with zwitterionic polymer brushes cannot be handled by the classical Hoffmeister series. More detailed investigations of ion distribution and water structure within the brush layers will help us not only understand but further improve the unique functions of zwitterionic polymer materials.

■ ASSOCIATED CONTENT

Supporting Information

The Supporting Information is available free of charge on the ACS Publications website at DOI: 10.1021/acs.jpcb.6b11540.

(1) Preparation of poly(sulfobetaine) brushes, (2) a phase shift image at boundary of polymer brush film and scratch track, (3) height fluctuation over time recorded in KCl, $N(CH_3)_4Cl$, $CaCl_2$, and sulfobetaine, (4) RICM snapshot, height fluctuations $\Delta h(t)$, normalized potential $V(\Delta h)/k_BT$, and autocorrelation function of height fluctuation of an "discocyte" measured in a physiological medium (PDF)

■ AUTHOR INFORMATION

Corresponding Authors

*E-mail: takahara@cstf.kyushu-u.ac.jp.

*E-mail: tanaka@uni-heidelberg.de.

ORCID

Motomu Tanaka: 0000-0003-3663-9554

Author Contributions

#These authors contributed equally. The manuscript was written through contributions of all authors. All authors have given approval to the final version of the manuscript. M.T. and A.T. conceived and directed the project. Y.H. and B.F. performed polymer brush preparation, RICM experiments and analyzed the results. A.Y. and R.M. performed RICM experiments with human erythrocytes experiments.

Notes

The authors declare no competing financial interest.

■ ACKNOWLEDGMENTS

This work was supported by MEXT (No. 26103521 to M.T.), JSPS (No. 26247070 to M.T., 26800223 and 16K05515 to A.Y., JP15H05761 to M.K.), EU FP7 (ActiveSoft), and German Science Foundation (SFB1129 and SFB873 to M.T.). M.T. is a member of German Cluster of Excellence "Cell Networks". I2CNER and iCeMS are supported by World Premier International Research Center Initiative (WPI), MEXT (Japan). Y.H. acknowledges the financial support of a Kyushu Univ. Short-Term International Research Exchange Program.

■ REFERENCES

(1) Van Deenen, L. Some Structural and Dynamic Aspects of Lipids in Biological Membranes. *Ann. N. Y. Acad. Sci.* **1966**, *137* (2), 717−730.

(2) Nelson, G. J. Lipid Composition of Erythrocytes in Various Mammalian Species. *Biochim. Biophys. Acta, Lipids Lipid Metab.* **1967**, *144* (2), 221−232.

(3) Chiu, D.; Lubin, B.; Roelofsen, B.; Van Deenen, L. Sickled Erythrocytes Accelerate Clotting in Vitro: An Effect of Abnormal Membrane Lipid Asymmetry. *Blood* **1981**, *58* (2), 398−401.

(4) Iwata, R.; Suk-In, P.; Hoven, V. P.; Takahara, A.; Akiyoshi, K.; Iwasaki, Y. Control of Nanobiointerfaces Generated from Well-Defined Biomimetic Polymer Brushes for Protein and Cell Manipulations. *Biomacromolecules* **2004**, *5* (6), 2308−2314.

(5) Schlenoff, J. B. Zwitteration: Coating Surfaces with Zwitterionic Functionality to Reduce Nonspecific Adsorption. *Langmuir* **2014**, *30* (32), 9625−9636.

(6) Shao, Q.; Jiang, S. Molecular Understanding and Design of Zwitterionic Materials. *Adv. Mater.* **2015**, *27* (1), 15−26.

(7) Shi, C.; Yan, B.; Xie, L.; Zhang, L.; Wang, J.; Takahara, A.; Zeng, H. Long-Range Hydrophilic Attraction between Water and Polyelectrolyte Surfaces in Oil. *Angew. Chem., Int. Ed.* **2016**, *55* (48), 15017−15021.

(8) Zhao, X.; Zhang, Z.; Pan, F.; Ma, Y.; Armes, S. P.; Lewis, A. L.; Lu, J. R. Solution pH-Regulated Interfacial Adsorption of Diblock Phosphorylcholine Copolymers. *Langmuir* **2005**, *21* (21), 9597−9603.

(9) Zhang, Z.; Chao, T.; Chen, S.; Jiang, S. Superlow Fouling Sulfobetaine and Carboxybetaine Polymers on Glass Slides. *Langmuir* **2006**, *22* (24), 10072−10077.

(10) Kobayashi, M.; Terayama, Y.; Kikuchi, M.; Takahara, A. Chain Dimensions and Surface Characterization of Superhydrophilic Polymer Brushes with Zwitterion Side Groups. *Soft Matter* **2013**, *9* (21), 5138−5148.

(11) Kobayashi, M.; Ishihara, K.; Takahara, A. Neutron Reflectivity Study of the Swollen Structure of Polyzwitterion and Polyeletrolyte Brushes in Aqueous Solution. *J. Biomater. Sci., Polym. Ed.* **2014**, *25* (14−15), 1673−1686.

(12) Wang, T.; Wang, X.; Long, Y.; Liu, G.; Zhang, G. Ion-Specific Conformational Behavior of Polyzwitterionic Brushes: Exploiting It for Protein Adsorption/Desorption Control. *Langmuir* **2013**, *29* (22), 6588−6596.

(13) Tairy, O.; Kampf, N.; Driver, M. J.; Armes, S. P.; Klein, J. Dense, Highly Hydrated Polymer Brushes via Modified Atom-Transfer-Radical-Polymerization: Structure, Surface Interactions, and Frictional Dissipation. *Macromolecules* **2015**, *48* (1), 140−151.

(14) Nomura, A.; Okayasu, K.; Ohno, K.; Fukuda, T.; Tsujii, Y. Lubrication Mechanism of Concentrated Polymer Brushes in Solvents: Effect of Solvent Quality and Thereby Swelling State. *Macromolecules* **2011**, *44* (12), 5013−5019.

(15) Kobayashi, M.; Takahara, A. Tribological Properties of Hydrophilic Polymer Brushes under Wet Conditions. *Chem. Records* **2010**, *10* (4), 208−216.

(16) Ishihara, K. Highly Lubricated Polymer Interfaces for Advanced Artificial Hip Joints through Biomimetic Design. *Polym. J.* **2015**, *47* (9), 585−597.

(17) Monzel, C.; Vaschgini, M.; Madsen, J.; Lewis, A. L.; Armes, S. P.; Tanaka, M. Fine Adjustment of Interfacial Potential between pH-Responsive Hydrogels and Cell-Sized Particles. *Langmuir* **2015**, *31* (31), 8689−8696.

(18) Kühner, M.; Sackmann, E. Ultrathin Hydrated Dextran Films Grafted on Glass: Preparation and Characterization of Structural,

DOI: 10.1021/acs.jpcb.6b11540
J. Phys. Chem. B 2017, 121, 1396−1404

Viscous, and Elastic Properties by Quantitative Microinterferometry. *Langmuir* **1996**, *12* (20), 4866−4876.
(19) Albersdörfer, A.; Sackmann, E. Swelling Behavior and Viscoelasticity of Ultrathin Grafted Hyaluronic Acid Films. *Eur. Phys. J. B* **1999**, *10* (4), 663−672.
(20) Tanaka, M.; Rehfeldt, F.; Schneider, M. F.; Mathe, G.; Albersdörfer, A.; Neumaier, K. R.; Purrucker, O.; Sackmann, E. Wetting and Dewetting of Extracellular Matrix and Glycocalix Models. *J. Phys.: Condens. Matter* **2005**, *17* (9), S649.
(21) Prieve, D. C.; Bike, S. G.; Frej, N. A. Brownian Motion of a Single Microscopic Sphere in a Colloidal Force Field. *Faraday Discuss. Chem. Soc.* **1990**, *90*, 209−222.
(22) Terayama, Y.; Kikuchi, M.; Kobayashi, M.; Takahara, A. Well-Defined Poly (sulfobetaine) Brushes Prepared by Surface-Initiated ATRP Using a Fluoroalcohol and Ionic Liquids as the Solvents. *Macromolecules* **2011**, *44* (1), 104−111.
(23) Murakami, R.; Tsai, C.-H. D.; Kaneko, M.; Sakuma, S.; Arai, F. Cell Pinball: Phenomenon and Mechanism of Inertia-Like Cell Motion in a Microfluidic Channel. *Lab Chip* **2015**, *15*, 3307−3313.
(24) Rädler, J. O.; Feder, T. J.; Strey, H. H.; Sackmann, E. Fluctuation Analysis of Tension-Controlled Undulation Forces between Giant Vesicles and Solid Substrates. *Phys. Rev. E: Stat. Phys., Plasmas, Fluids, Relat. Interdiscip. Top.* **1995**, *51* (5), 4526−4536.
(25) Reynolds, O. An Experimental Investigation of the Circumstances which Determine whether the Motion of Water shall be Direct or Sinuous, and of the Law of Resistance in Parallel Channels. *Proc. R. Soc. London* **1883**, *35* (224-226), 84−99.
(26) Pincus, P. Colloid Stabilization with Grafted Polyelectrolytes. *Macromolecules* **1991**, *24* (10), 2912−2919.
(27) Derjaguin, B. V. Some Results from 50 Years' Research on Surface Forces. In *Surface Forces and Surfactant Systems*; Springer: Berlin Heidelberg, 1987; pp 17−30.
(28) Swain, P. S.; Andelman, D. The Influence of Substrate Structure on Membrane Adhesion. *Langmuir* **1999**, *15* (26), 8902−8914.
(29) Hofmeister, F. Zur Lehre von der Wirkung der Salze. *Naunyn-Schmiedeberg's Arch. Pharmacol.* **1888**, *24* (4), 247−260.
(30) Herrmann, M.; Schneck, E.; Gutsmann, T.; Brandenburg, K.; Tanaka, M. Bacterial Lipopolysaccharides form Physically Cross-Linked, Two-Dimensional Gels in the Presence of Divalent Cations. *Soft Matter* **2015**, *11* (30), 6037−6044.
(31) Higaki, Y.; Kobayashi, M.; Murakami, D.; Takahara, A. Anti-Fouling Behavior of Polymer Brush Immobilized Surfaces. *Polym. J.* **2016**, *48* (4), 325−331.
(32) Blakeston, A. C.; Alswieleh, A. M.; Heath, G. R.; Roth, J. S.; Bao, P.; Cheng, N.; Armes, S. P.; Leggett, G. J.; Bushby, R. J.; Evans, S. D. New Poly(amino acid methacrylate) Brush Supports the Formation of Well-Defined Lipid Membranes. *Langmuir* **2015**, *31* (12), 3668−3677.
(33) Morita, S.; Tanaka, M.; Ozaki, Y. Time-Resolved In Situ ATR-IR Observations of the Process of Sorption of Water into a Poly(2-methoxyethyl acrylate) Film. *Langmuir* **2007**, *23* (7), 3750−3761.
(34) Murakami, D.; Kobayashi, M.; Moriwaki, T.; Ikemoto, Y.; Jinnai, H.; Takahara, A. Spreading and Structuring of Water on Super-hydrophilic Polyelectrolyte Brush Surfaces. *Langmuir* **2013**, *29* (4), 1148−1151.
(35) Zilker, A.; Ziegler, M.; Sackmann, E. Spectral Analysis of Erythrocyte Flickering in the 0.3−4-μm^{-1} Regime by Microinterferometry Combined with Fast Image Processing. *Phys. Rev. A: At., Mol., Opt. Phys.* **1992**, *46* (12), 7998−8001.
(36) Agre, P.; Casella, J. F.; Zinkham, W. H.; McMillan, C.; Bennett, V. Partial Deficiency of Erythrocyte Spectrin in Hereditary Spherocytosis. *Nature* **1985**, *314* (6009), 380−383.

DOI: 10.1021/acs.jpcb.6b11540
J. Phys. Chem. B 2017, 121, 1396−1404